# Microbiota-Generated Metabolites Promote Metabolic Benefits via Gut-Brain Neural Circuits

Filipe De Vadder,[1,2,3] Petia Kovatcheva-Datchary,[4] Daisy Goncalves,[1,2,3] Jennifer Vinera,[1,2,3] Carine Zitoun,[1,2,3] Adeline Duchampt,[1,2,3] Fredrik Bäckhed,[4,5] and Gilles Mithieux[1,2,3,*]

[1]Institut de la Santé et de la Recherche Médicale, U855, Lyon 69372, France
[2]Université de Lyon, Lyon 69008, France
[3]Université Lyon 1, Villeurbanne 69622, France
[4]Wallenberg Laboratory and Department of Molecular and Clinical Medicine, University of Gothenburg 41345, Sweden
[5]Novo Nordisk Foundation Center for Basic Metabolic Research, Section for Metabolic Receptology and Enteroendocrinology, Faculty of Health Sciences, University of Copenhagen, Copenhagen 2200, Denmark
*Correspondence: gilles.mithieux@inserm.fr
http://dx.doi.org/10.1016/j.cell.2013.12.016

## SUMMARY

Soluble dietary fibers promote metabolic benefits on body weight and glucose control, but underlying mechanisms are poorly understood. Recent evidence indicates that intestinal gluconeogenesis (IGN) has beneficial effects on glucose and energy homeostasis. Here, we show that the short-chain fatty acids (SCFAs) propionate and butyrate, which are generated by fermentation of soluble fiber by the gut microbiota, activate IGN via complementary mechanisms. Butyrate activates IGN gene expression through a cAMP-dependent mechanism, while propionate, itself a substrate of IGN, activates IGN gene expression via a gut-brain neural circuit involving the fatty acid receptor FFAR3. The metabolic benefits on body weight and glucose control induced by SCFAs or dietary fiber in normal mice are absent in mice deficient for IGN, despite similar modifications in gut microbiota composition. Thus, the regulation of IGN is necessary for the metabolic benefits associated with SCFAs and soluble fiber.

## INTRODUCTION

Extrinsic factors such as a sedentary lifestyle and excessive caloric intake contribute to the increasing incidence of obesity and type 2 diabetes. It is well-established that diet quality can be improved by reducing the intake of fat and simple sugars while increasing the intake of dietary fiber. Dietary fiber is the indigestible portion of plant foods and has two main components: insoluble fiber (principally cellulose and lignin) and soluble fiber such as galacto-oligosaccharides and fructo-oligosaccharides (FOS), which are fermented by the gut microbiota into short-chain fatty acids (SCFAs) acetate, propionate, and butyrate (Flint et al., 2012). Fiber-enriched diets improve insulin sensi-

tivity and glucose tolerance in lean (Robertson et al., 2003, 2005) and obese diabetic subjects (Mendeloff, 1977; Ray et al., 1983).

The beneficial effects of soluble fiber are often considered to be mediated by SCFAs through regulation of whole-body energy homeostasis (Layden et al., 2013). SCFAs are also signaling molecules, acting not only as important modulators of the epigenome through altering histone acetylation but also as endogenous ligands for the G-protein-coupled receptors FFAR3 and FFAR2 (Brown et al., 2003). Signaling through these receptors mediates numerous effects such as synthesis of glucagon-like peptide 1 in enteroendocrine cells (Tolhurst et al., 2012), modulation of adiposity, and changes in gut transit time (Samuel et al., 2008). In some aspects, the benefits of soluble fiber on glucose and energy homeostasis appear paradoxical. First, butyrate is a key energy substrate for both colonocytes and enterocytes (Donohoe et al., 2011). How could an increase in energy harvest be reconciled with a benefit on energy homeostasis? Recent studies have described a role of butyrate in enhancing energy expenditure (Gao et al., 2009; Lin et al., 2012), but mechanistic insights into how this is achieved are less understood. Second, propionate is classically described as an efficient hepatic gluconeogenic substrate (Anderson and Bridges, 1984). An increase in hepatic glucose production is recognized as a causal factor of insulin resistance (Clore et al., 2000; Magnusson et al., 1992), leading to type 2 diabetes, and thus it is unclear how this could be reconciled with a metabolic benefit of soluble fibers.

It is noteworthy that most studies featuring propionate as a gluconeogenic substrate were carried out before the intestine was described as a gluconeogenic organ (Croset et al., 2001; Mithieux et al., 2004a; Rajas et al., 1999). Studies from our lab suggest that intestinal gluconeogenesis (IGN) induces beneficial effects on glucose and energy homeostasis. We have shown that glucose released by IGN is detected by a portal vein glucose sensor that transmits its signal to the brain by the peripheral nervous system to promote beneficial effects on food intake and glucose metabolism (Delaere et al., 2012). This chain of events is of particular relevance with protein-enriched diets
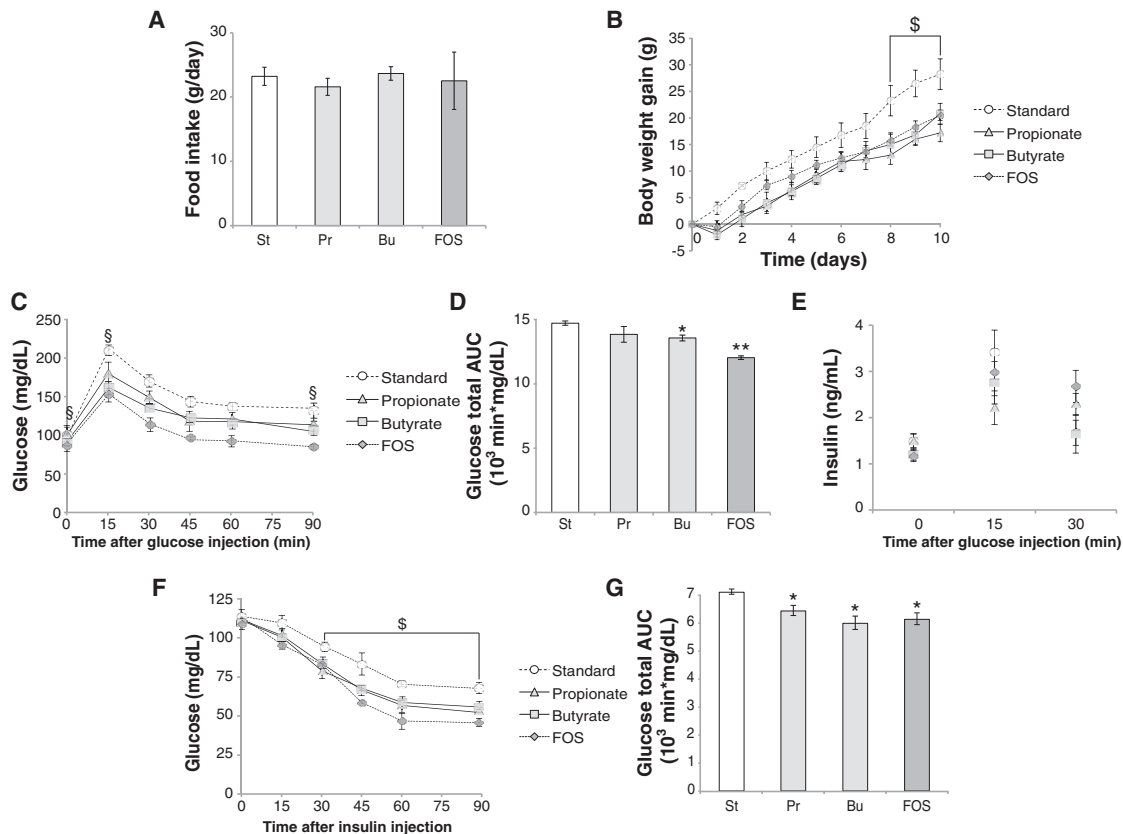
**Figure 1. Effects of Dietary SCFAs and FOS on Body Weight and Glucose Homeostasis in Rats**

(A–G) Food intake (A) and body weight gain (B) of rats fed standard or butyrate-, propionate- or FOS-enriched diet. Glucose (C) and insulin (F) tolerance tests were performed respectively 11 and 13 days after switching to the indicated diets. Blood glucose levels and total glucose area under the curve (AUC) (D and G) are shown. (E) Insulin plasma levels were determined in samples taken during the glucose tolerance test. \$, p < 0.05 standard versus all groups; §, p < 0.05 standard versus butyrate and FOS; *p < 0.05 versus standard; **p < 0.01 versus standard (ANOVA followed by Dunnett's post hoc test). Data are mean ± SEM, n = 6 rats per group. St, standard; Pr, propionate; Bu, butyrate; FOS, fructo-oligosaccharides. See also Figure S1.

(Duraffourd et al., 2012; Mithieux et al., 2005; Pillot et al., 2009) and after gastric bypass surgery (Troy et al., 2008). We hypothesized that propionate is a substrate of IGN because its downstream metabolites enter the gluconeogenic pathway via the citric acid cycle, which is the main route of glucose formation in the small intestine (Croset et al., 2001; Mithieux et al., 2004b), and because propionate is produced in the gut lumen.

Renewed interest in SCFAs has emerged because of the recently identified association between gut microbiota composition and obesity and associated pathologies (Flint et al., 2012). Microbiota from obese individuals might have a higher capacity for energy harvest than those from lean individuals (Schwiertz et al., 2010; Turnbaugh et al., 2009a), and several studies have shown a major influence of high-fat diets on the composition of gut microbiota in rodents (Hildebrandt et al., 2009; Parks et al., 2013; Turnbaugh et al., 2008, 2009b). Furthermore, a recent study in obese humans indicates that specific microbiota compositions may be associated with impaired glucose control (Karlsson et al., 2013).

Here we combined gene expression and metabolic tracer studies to evaluate whether soluble fiber and/or SCFAs could induce intestinal glucose production, either by regulating gluconeogenic gene expression, or, for propionate, by serving as a substrate. We also tested whether IGN might account for the benefits of soluble fiber, and specifically whether it had a causal role in the protection against diet-induced deregulation of glucose homeostasis. Finally, using mice with an intestinal-specific knockout of the catalytic subunit (G6pc) of glucose-6-phosphatase (G6Pase, the essential enzyme of gluconeogenesis), we evaluated the respective roles of the host IGN function and the gut microbiota composition in the metabolic benefits conferred by the presence of soluble fiber in the diet.

## RESULTS

### Dietary SCFAs and FOS Increase Glucose Tolerance and Insulin Sensitivity in Rats

We first confirmed the beneficial effects of SCFAs (propionate and butyrate) and FOS on body weight gain in rats. Body weight of rats on a standard diet increased by 30 ± 2.5 g over 10 days; despite a similar food intake, SCFA- and FOS-fed rats showed significantly less weight gain over this time period (Figures 1A
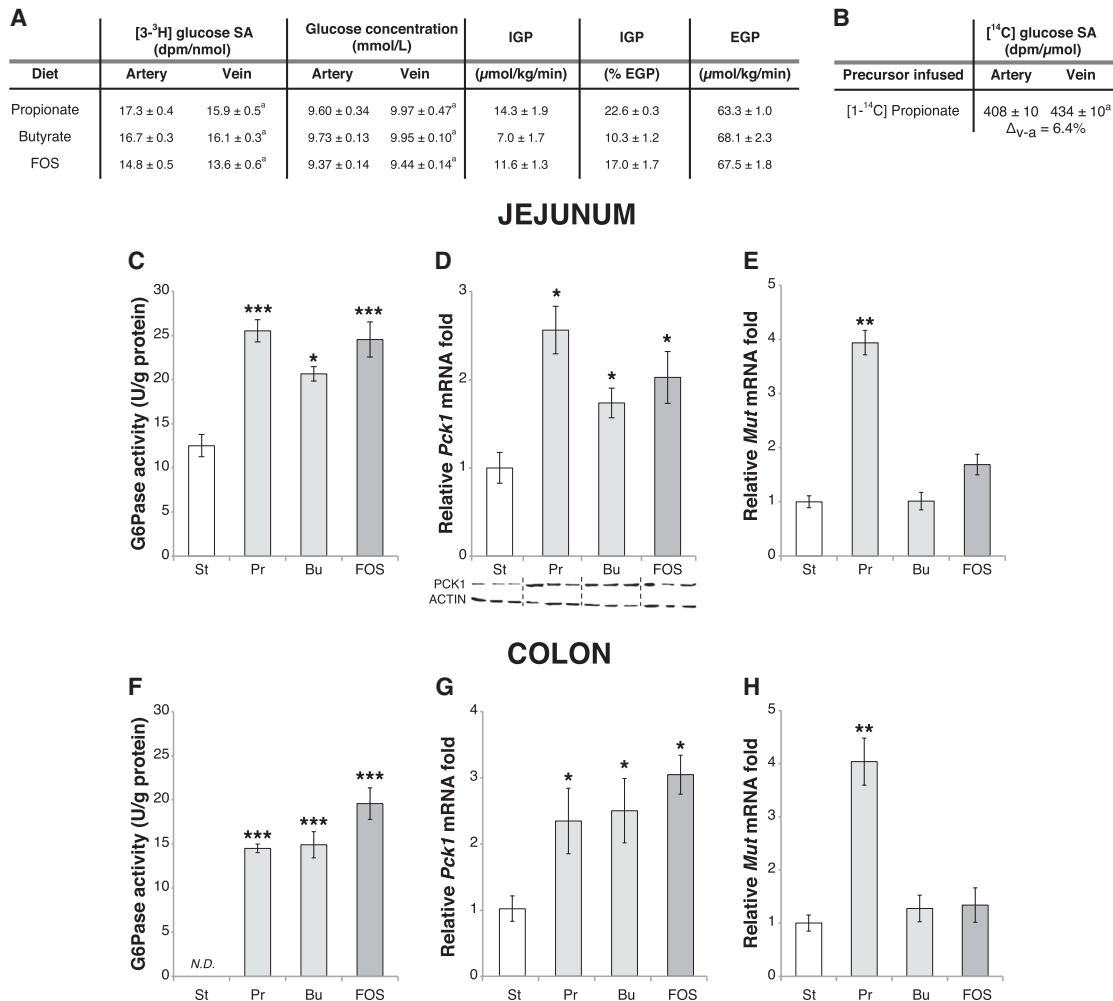
| Diet | [3-$^3$H] glucose SA (dpm/nmol) | | Glucose concentration (mmol/L) | | IGP ($\mu$mol/kg/min) | IGP (% EGP) | EGP ($\mu$mol/kg/min) |
|---|---|---|---|---|---|---|---|
| | Artery | Vein | Artery | Vein | | | |
| Propionate | 17.3 ± 0.4 | 15.9 ± 0.5[a] | 9.60 ± 0.34 | 9.97 ± 0.47[a] | 14.3 ± 1.9 | 22.6 ± 0.3 | 63.3 ± 1.0 |
| Butyrate | 16.7 ± 0.3 | 16.1 ± 0.3[a] | 9.73 ± 0.13 | 9.95 ± 0.10[a] | 7.0 ± 1.7 | 10.3 ± 1.2 | 68.1 ± 2.3 |
| FOS | 14.8 ± 0.5 | 13.6 ± 0.6[a] | 9.37 ± 0.14 | 9.44 ± 0.14[a] | 11.6 ± 1.3 | 17.0 ± 1.7 | 67.5 ± 1.8 |

**A**

**B**

| Precursor infused | [$^{14}$C] glucose SA (dpm/$\mu$mol) | |
|---|---|---|
| | Artery | Vein |
| [1-$^{14}$C] Propionate | 408 ± 10 | 434 ± 10[a] |
| | $\Delta_{v-a}$ = 6.4% | |



JEJUNUM

COLON

Figure 2. Effect of Dietary SCFAs and FOS on IGN in Rats

(A) Endogenous glucose production (EGP) and intestinal glucose fluxes were determined in rats fed a standard, butyrate-, propionate-, or FOS-enriched diet for 2 weeks.

(B) Determination of intestinal incorporation of $^{14}$C-labeled propionate into glucose in 24-hr-fasted rats. [a]Different from value in artery (p < 0.05, Student's two-tailed test for paired values). SA, specific activity.

(C–H) G6Pase activity and *Pck1* and *Mut* expression were evaluated in the jejunum (C to E) and colon (F to H) of rats fed the indicated diets. *p < 0.05; **p < 0.01; ***p < 0.001 versus standard (ANOVA followed by Dunnett's post hoc test).

Data are mean ± SEM of n = 6 rats per group. St, standard; Pr, propionate; Bu, butyrate; FOS, fructo-oligosaccharides; N.D., not detected.

and 1B). Importantly, SCFAs and FOS did not influence fat absorption by the gastrointestinal tract (data not shown). To confirm that SCFAs and FOS also improve glucose homeostasis, we performed intraperitoneal glucose (GTT) and insulin (ITT) tolerance tests. The SCFA- and FOS-fed rats exhibited improved glucose tolerance compared with rats fed a standard diet (Figures 1C and 1D), with no associated increase of insulin secretion (Figure 1E). In addition, basal glucose levels after a 16 hr fast were about 15% lower in butyrate- and FOS-fed rats compared with rats fed a standard diet (Figure 1C, time 0). Similarly, insulin tolerance was significantly enhanced in the SCFA- and FOS-fed rats (Figures 1F and 1G). Furthermore, hepatic G6Pase activity was lower in FOS-fed rats compared with rats on a standard diet (Figure S1 available online), which was in line with the

improvement of glucose control, as previously observed after IGN induction by gastric bypass surgery (Troy et al., 2008).

### Dietary SCFAs and FOS Induce Intestinal Glucose Production and IGN Gene Expression

We next quantified intestinal glucose production (IGP) in rats fed propionate, butyrate or FOS for 2 weeks. In all three groups, [3-$^3$H] glucose specific activity was lower in the portal vein than in the artery (Figure 2A). This indicated that newly synthesized, unlabeled glucose had been released by the intestine. Moreover, plasma glucose concentrations were slightly higher in the portal vein than in the artery (Figure 2A), indicating that IGP was able to counterbalance intestinal glucose utilization. Of note, propionate had the strongest capacity to induce IGP,
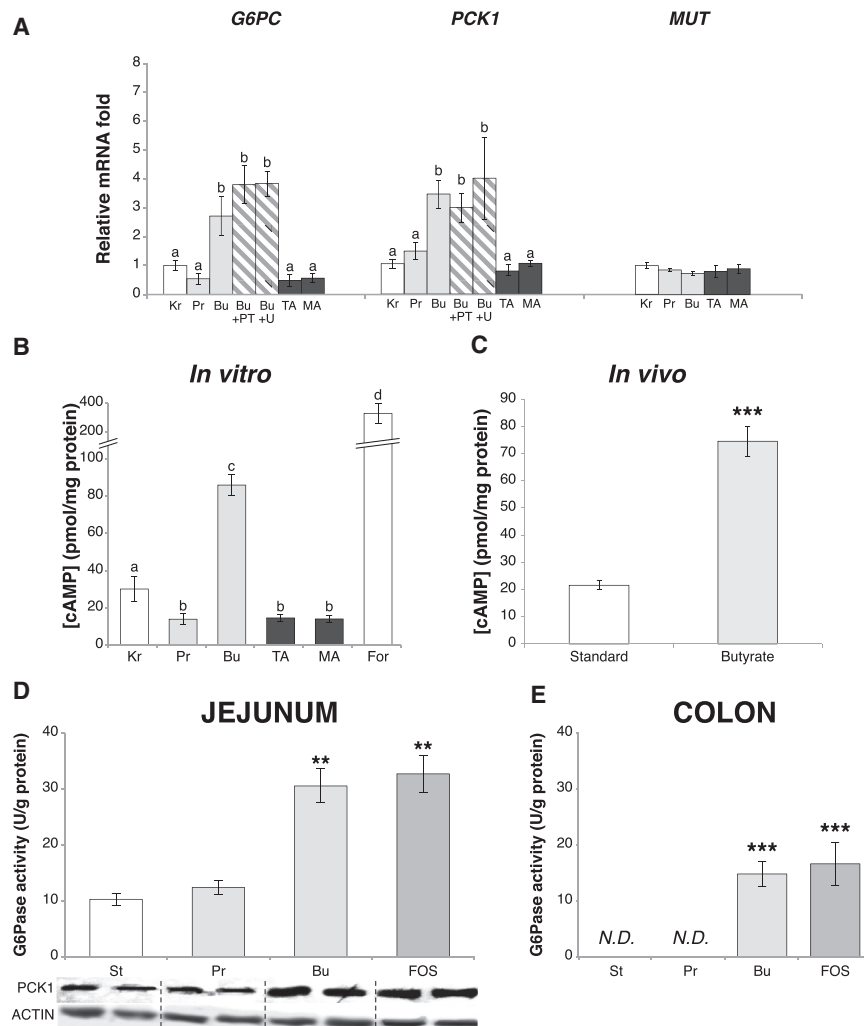
**Figure 3. Butyrate Directly Activates IGN Genes, Whereas Propionate Action Is Dependent on the Integrity of Periportal Afferents**

(A and B) Caco-2 cells were cultured at confluence for 3 weeks and mRNA levels of *G6PC, PCK1* and *MUT* were evaluated using quantitative RT-PCR (A) and intracellular cAMP was measured (B). Kr, Krebs-Ringer; Pr, propionate; Bu, butyrate; PT, pertussis toxin; U, U73122; TA, tiglic acid; MA, 1-methylcyclopropanecarboxylic acid; For, forskolin. Values with different letters differ significantly ($p < 0.05$, ANOVA followed by Tukey's post hoc test). n = 9 wells per experimental group.

(C) Rats were fed standard or butyrate-enriched diet for two weeks and cAMP content was measured in the jejunum.

(D and E) G6Pase activity and PCK1 protein expression were analyzed in the jejunum (D) and colon (E) of capsaicin-treated animals fed the indicated diets. **$p < 0.01$; ***$p < 0.001$ versus standard (ANOVA followed by Dunnett's post hoc test). Data are mean ± SEM, n = 6 rats per group. St, standard; Pr, propionate; Bu, butyrate; FOS, fructo-oligosaccharides; N.D., not detected. See also Figure S2.

of rats fed a standard diet (Figure 2F). The pattern of induction of *Pck1* and *Mut* expression in the colon in response to SCFAs and FOS was similar to that observed in the jejunum (Figures 2G and H).

**Butyrate but Not Propionate Is Able to Directly Induce IGN Genes**

We next investigated if SCFAs could directly induce IGN genes using Caco-2 cells, which have a phenotype that resembles the enterocytes of the small intestine (Hidalgo et al., 1989). Expression of *G6PC*, *PCK1*, and *MUT* in Caco-2 cells was not affected by 24 hr incubation with propionate or specific agonists of FFAR2 (tiglic acid [TA]) or FFAR3 (1-methylcyclopropanecarboxylic acid [MA]) (Schmidt et al., 2011) (Figure 3A). However, expression of *G6PC* and *PCK1* was increased 2- to 3-fold in cells incubated with butyrate (Figure 3A). Neither pertussis toxin nor U73122 (inhibitors of Gi- and Gq-mediated signaling, respectively) was able to counterbalance the effect of butyrate (Figure 3A, dashed bars), indicating that induction of *G6PC* and *PCK1* expression by butyrate was not dependent on any Gi- or Gq-mediated mechanism. Intracellular cAMP content was increased 3-fold in butyrate-treated cells compared with control cells, while no cAMP increase was observed in cells treated with propionate, TA, or MA (Figure 3B). Interestingly, a similar cAMP increase was observed in the jejunum of rats fed a butyrate-enriched diet (Figure 3C). These data suggest that butyrate-mediated induction of *G6PC* and *PCK1* gene expression could be mediated by cAMP, a known activator of these genes (Gautier-Stein et al., 2006; Mutel et al., 2011).

accounting for 23% of total endogenous glucose production (Figure 2A). We therefore investigated whether [$^{14}$C]-propionate carbons could be incorporated into newly synthesized glucose. [$^{14}$C]-glucose specific activity after a 24 hr fast was significantly higher in portal venous blood than in arterial blood (Figure 2B), suggesting that the small intestine is able to efficiently convert propionate into glucose.

We then studied the effect of SCFA- and FOS-enriched diets on G6Pase activity and IGN gene expression. Rats fed SCFAs or FOS for 2 weeks had about 2-fold higher G6Pase activity in the jejunum compared with rats fed a standard diet (Figure 2C); similar increases in both mRNA and protein levels of phosphoenolpyruvate carboxykinase (cytosolic form, *Pck1*) in response to SCFAs and FOS were also observed (Figure 2D). Interestingly, only propionate induced the expression of methylmalonyl-coA mutase (*Mut*), the key enzyme for its incorporation into glucose (Figure 2E). In rats fed SCFAs or FOS for 2 weeks, there was a dramatic induction of G6Pase activity in the colon (where the microbiota produces SCFAs in greatest concentrations), resulting in an activity similar to that observed in the jejunum of rats fed a standard diet; G6Pase activity was not detected in the colon

## Propionate Induction of IGN Depends on Gut-Brain Neural Communication

Since only butyrate can directly activate IGN genes in vitro, we hypothesized that propionate-mediated induction of IGN could depend upon a gut-brain communication axis. To question the role of the portal neural afferents in the induction of IGN gene expression by propionate, we performed periportal nervous deafferentiation with capsaicin in rats before feeding with SCFAs- and FOS-enriched diets for 2 weeks. G6Pase activity and PCK1 protein expression were not increased in the intestine of capsaicin-treated rats fed propionate compared with the expression in rats fed a standard diet (Figures 3D and 3E). By contrast, dietary butyrate and FOS could still increase G6Pase activity and PCK1 expression in capsaicin-treated rats (Figures 3D and 3E). However, these responses were clearly not associated with improvements in glucose homeostasis since the beneficial effects of dietary SCFAs and FOS on body weight gain and improvement in glucose and insulin tolerance were abolished by denervation (Figures S2A–S2E). These results are consistent with the crucial role of the periportal nervous system in transducing the beneficial effects of IGN and portal glucose sensing (Mithieux et al., 2005; Troy et al., 2008). Moreover, no inhibition of G6Pase activity was observed in the liver of capsaicin-treated rats fed SCFAs or FOS; in fact, a slight increase was observed in propionate-fed animals (Figure S2F).

Since the propionate receptor FFAR3 is expressed in the peripheral nervous system (Kimura et al., 2011; Nøhr et al., 2013), we used immunofluorescence studies to examine the presence of FFAR3 in the nerve fibers of the portal vein. As shown in Figure 4A, the neuronal marker PGP9.5 (left) and FFAR3 (right) were expressed in the rat portal vein wall and found in close proximity (bottom, in yellow).

Next, we tested whether propionate-induced IGN activation depended on FFAR3 signaling in vivo. When propionate was infused in the portal vein at a rate mimicking that of a FOS-enriched meal, G6Pase activity showed a 2.5-fold increase in the jejunum when compared to the activity level after a saline infusion (Figure 4B). In contrast, the ketone body β-hydroxybutyrate (β-HB), an antagonist of FFAR3 (Kimura et al., 2011), induced a slight decrease in G6Pase activity when infused alone and reversed the propionate-mediated induction when infused together with propionate (Figure 4B).

Lastly, we evaluated the impact of propionate feeding on the regions of the central nervous system implicated in signaling from the portal area: the dorsal vagal complex (DVC), which receives inputs from the vagal pathway, the C1 segment of the spinal cord and the parabrachial nucleus (PBN), which receive inputs from the spinal pathway, and the hypothalamus, which receives inputs from both the PBN and the DVC (Berthoud, 2004). Dietary propionate caused a 2- to 3-fold induction of c-Fos (a well-recognized marker of neuronal activation; Sagar et al., 1988) in all areas of the DVC (Figures 4C–4E), as well as in the spinal C1 segment and the PBN (Figures S3A–S3D). Interestingly, such activation was absent in capsaicin-treated rats (Figures 4D and 4F). A similar pattern of c-Fos activation (and of denervation effect) occurred in the main hypothalamic regions, which receive inputs from both the PBN and the DVC, namely the paraventricular nucleus (PVN), the lateral hypothalamus (LH) and the arcuate nucleus (ARC) (Figures S3E–S3H).

Taken together, these data suggest that FFAR3 is a major actor in the gut-brain communication mechanism leading to propionate-mediated induction of IGN.

## IGN Plays a Causal Role in SCFA- and FOS-Induced Metabolic Benefits under Both Normal and Insulin-Resistant Conditions

To determine whether IGN has a causal role in SCFA- and FOS-induced metabolic improvements, we used mice deficient in IGN (i.e., with specific disruption of the G6Pase catalytic subunit in the intestine, I-G6pc−/− mice, Penhoat et al., 2011). When fed SCFA- or FOS-enriched diets, wild-type (WT) mice exhibited the same metabolic benefits as those observed in rats, i.e., enhanced glucose and insulin tolerance (Figure 5, left). In contrast, these metabolic benefits were not observed in I-G6pc−/− mice (Figure 5, right), and glucose tolerance was even slightly impaired in I-G6pc−/− mice fed a propionate-enriched diet (Figures 5B and 5D). We observed no differences in body weight gain on standard diet (data not shown) or food intake between I-G6pc−/− and WT mice (Figure S4A). Furthermore, when compared to WT mice, body weight gain in I-G6pc−/− mice was significantly higher after switching to SCFA- and FOS-enriched diets (Figure S4B).

To elucidate the role of IGN in the well-known FOS-mediated resistance to diet-induced obesity and deregulation of glucose control, we fed WT and I-G6pc−/− mice a high-fat/high-sucrose (HF-HS) diet (composition available in Table S1) with or without FOS. In WT mice, addition of FOS to a HF-HS diet abolished the development of diet-induced obesity without an effect on food intake (Figures 6A and 6B), dramatically improved glucose and insulin tolerance (Figures 6C–6F), and significantly decreased fat mass in the subcutaneous, epididymal and visceral adipose tissues (Figures S5A–S5C). In contrast, in I-G6pc−/− mice fed a HF-HS diet, FOS supplementation resulted in increased body weight (Figure 6A), no change in glucose tolerance (Figures 6C and 6D), decreased insulin tolerance (Figures 6E and 6F), and no change in fat mass in the subcutaneous and visceral adipose tissues (Figures S5A–S5C). Thus, the FOS-mediated resistance to diet-induced obesity and improvement of glucose control was absent in I-G6pc−/− mice. In fact, these mice experienced increased body weight gain and worsened insulin tolerance in response to FOS supplementation.

We used two-way ANOVA to evaluate the relative effects of genotype and diet on the total observed variability between WT and I-G6pc−/− mice on a HF-HS diet with or without FOS. Regarding glucose tolerance and insulin sensitivity, there was a strong interaction between diet and genotype (p = 0.0261 for GTT; p = 0.0004 for ITT), with genotype accounting for almost 50% of the total variance. This strong effect of genotype was also found for adiposity (29.43% of variance, p = 0.0017 in visceral adipose tissue), suggesting that IGN accounts for most of the metabolic improvements observed in FOS feeding. Moreover, intestinal G6Pase activity was induced in FOS-fed WT mice, whereas only residual nonspecific activity
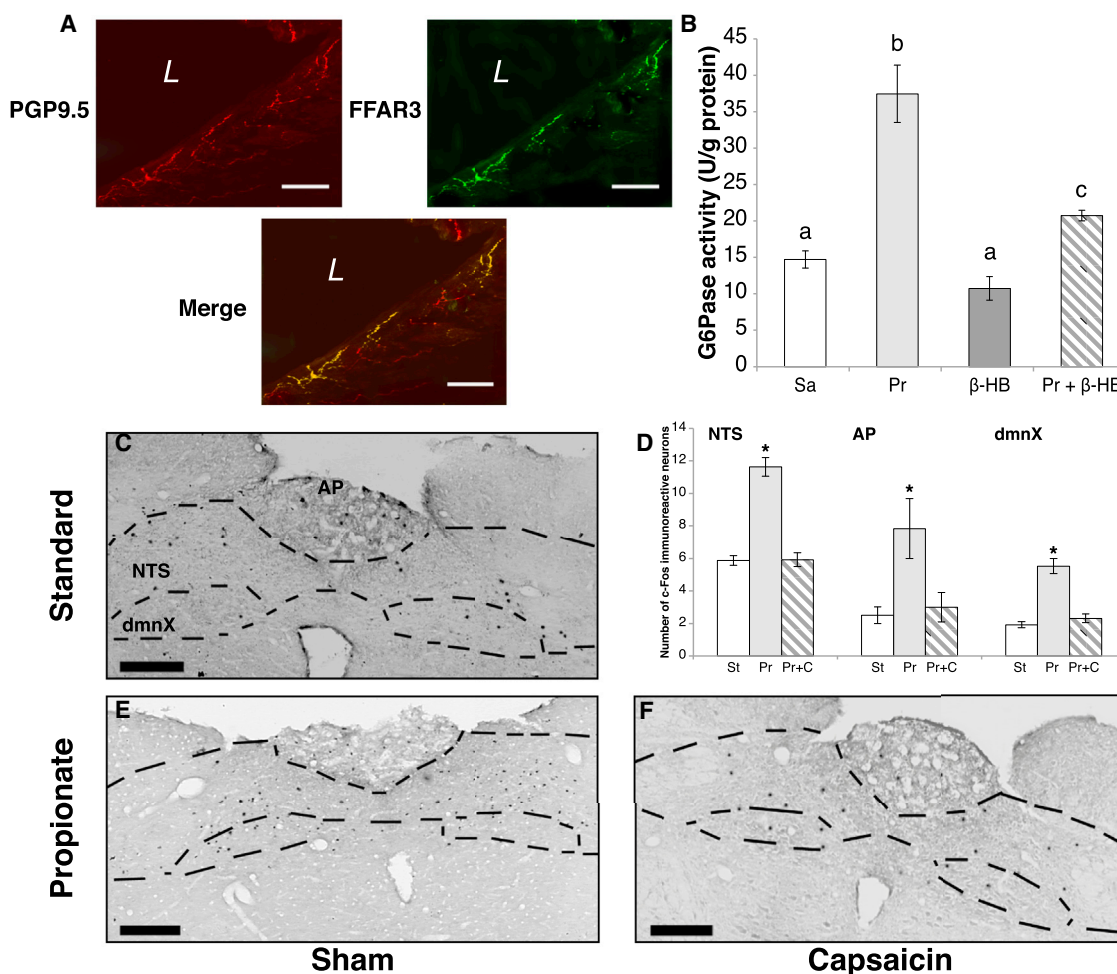
**Figure 4. Propionate Initiates a Gut-Brain Circuit Dependent on FFAR3 in the Portal Nerves**

(A) Neuronal marker PGP9.5 (red, left) colocalized with FFAR3 (green, right) in the walls of the portal vein of rats. Lower, merged image. Scale bar, 50 μm. L, vein lumen.

(B) G6Pase activity in the jejunum of rats after a 6 hr-perfusion of saline (Sa), propionate (Pr) or β-hydroxybutyrate (β-HB). Values with different letters differ significantly ($p < 0.05$, one-way ANOVA followed by Tukey's post hoc test). Data are mean ± SEM, n = 5 rats per group.

(C, E and F) c-Fos immunoreactive cells in the DVC of rats fed standard (C) or propionate-enriched diet, after treatment of the portal area with vehicle (E) or capsaicin (F).

(D) Quantification of c-Fos neurons in all areas of the DVC.

St, standard, Pr, propionate, Pr+C, propionate + capsaicin. AP, area postrema; NTS, nucleus of the solitary tract; dmnX, dorsal motor nucleus of the vagus. Scale bar, 200 μm. Data are mean ± SEM per hemisphere, on 4 to 6 sections per area, n = 3 rats per group. *$p < 0.05$ versus all groups (Kruskal-Wallis test followed by Dunn's post hoc test). See also Figure S3.

was observed in I-G6pc−/− mice (Figure 6G). We also observed a weak decrease in hepatic G6Pase activity ($p = 0.07$) accompanied by dramatic increases in liver glucose-6-phosphate (G6P) and glycogen content in FOS-fed WT mice (Figures S5D–S5F), suggesting a suppression of hepatic glucose release. By contrast, FOS supplementation did not induce a change in the parameters of hepatic glucose release in I-G6pc−/− mice (Figures S5D–S5F). Again, there was a strong interaction between diet and genotype accounting for FOS feeding-induced changes in these parameters (e.g., 26.94% of total variance, $p < 0.0001$ for liver G6P content). Taken together, these data strongly suggest that IGN plays a

mandatory role in the beneficial metabolic effects of SCFA- and FOS-enriched diets.

## FOS Feeding Induces a Genotype-Independent Shift in the Microbiota Composition

Diet is a major factor that drives gut microbiota composition and its fermentative capacity. To investigate how FOS supplementation of HF-HS diet affected the colonic microbial ecology in WT and I-G6pc−/− mice, we performed 454-based pyrosequencing. By estimating β-diversity between samples with pairwise unweighted Unifrac distance (Lozupone and Knight, 2005) and performing principal coordinates analysis, we found that
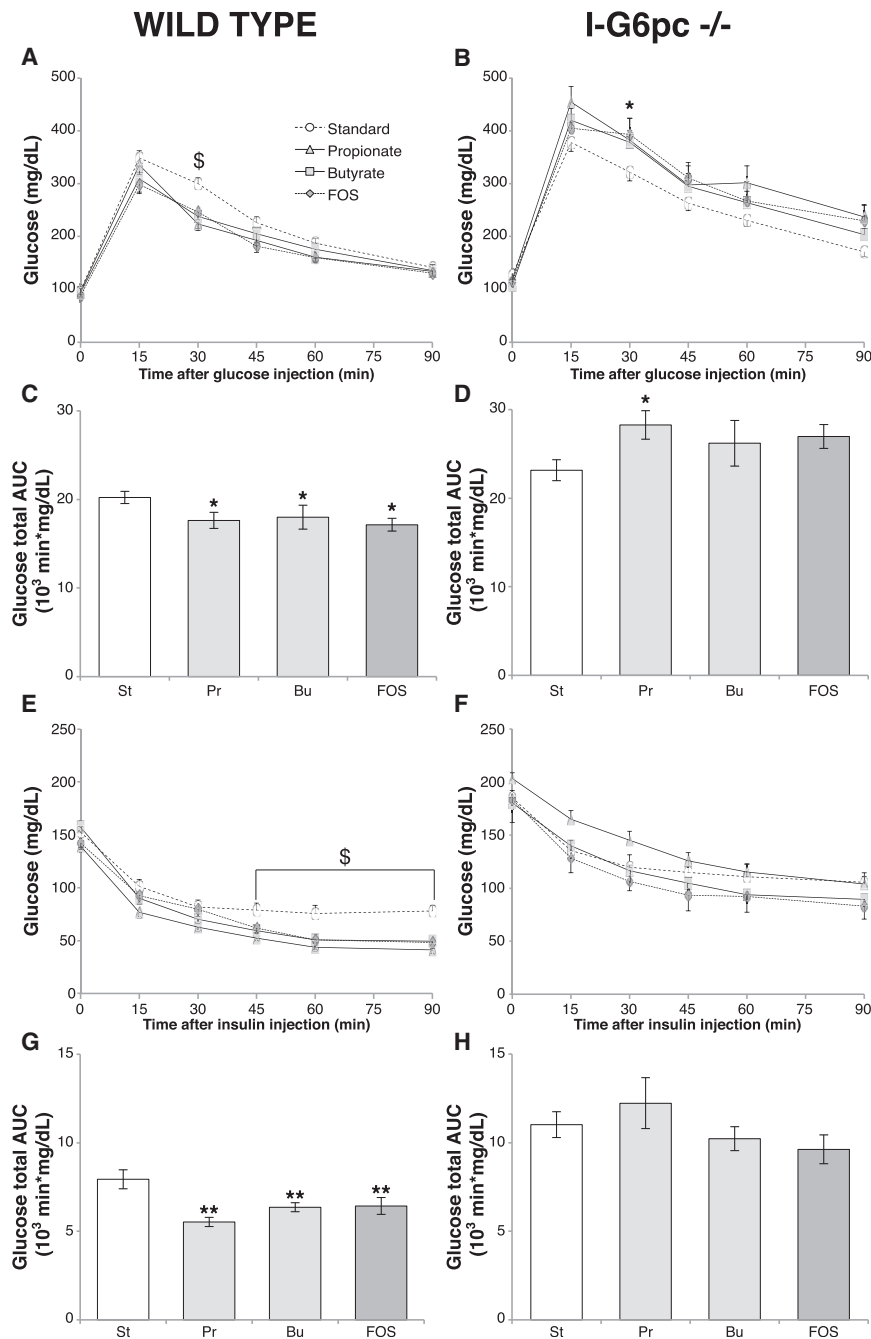
# WILD TYPE

# I-G6pc -/-

only in I-G6pc−/− mice (Figure 7E), with a significant interaction between diet and genotype (two-way ANOVA, p = 0.0155).

To assess the metabolic consequences of FOS incorporation in the diet, we measured total SCFA content in portal and peripheral blood from WT and I-G6pc−/− mice. As expected, total SCFA content was higher in portal blood after FOS supplementation, with diet accounting for almost 60% of the variance (p = 0.001, two-way ANOVA) and no influence of the mouse genotype (p = 0.66, two-way ANOVA) (Figure 7F). Butyrate proportions did not vary in any of the groups (Figure 7G). However, the contribution of propionate to the total content of SCFAs in portal blood increased with FOS supplementation in I-G6pc−/− mice but not in WT mice (Figure 7G); this result is consistent with the assumption that propionate is used as a substrate of gluconeogenesis in the gut of WT but not I-G6pc−/− mice. Notably, the abundance of Bacteroidetes positively correlated with the changes in portal blood propionate (Figure 7H, $R^2$ = 0.53, p =

diet had a profound effect on the ecology in both genotypes (Figure 7A). The changes associated with diet (PC1, 41%) were preponderant compared to those associated with genotype (PC2, 11%). Firmicutes and Bacteroidetes were the most abundant phyla, representing more than 80% of the reads (Figure 7B). Diet had a major effect on the relative abundance of the main phyla in the colonic microbiota and FOS feeding was associated with a significant decrease in Firmicutes and increase in Bacteroidetes in both WT and I-G6pc−/− mice (Figures 7C and 7D). Actinobacteria abundance was significantly increased by FOS

0.0002). No significant variation of SCFA content was observed in peripheral blood (Figure S6), which is consistent with the fact that most SCFAs are metabolized by the liver (Cummings et al., 1987).

## DISCUSSION

Here we examined the metabolic activities of SCFAs and FOS, focusing particularly on IGN, a regulator of glucose and energy homeostasis (Mithieux et al., 2005; Troy et al., 2008). We found
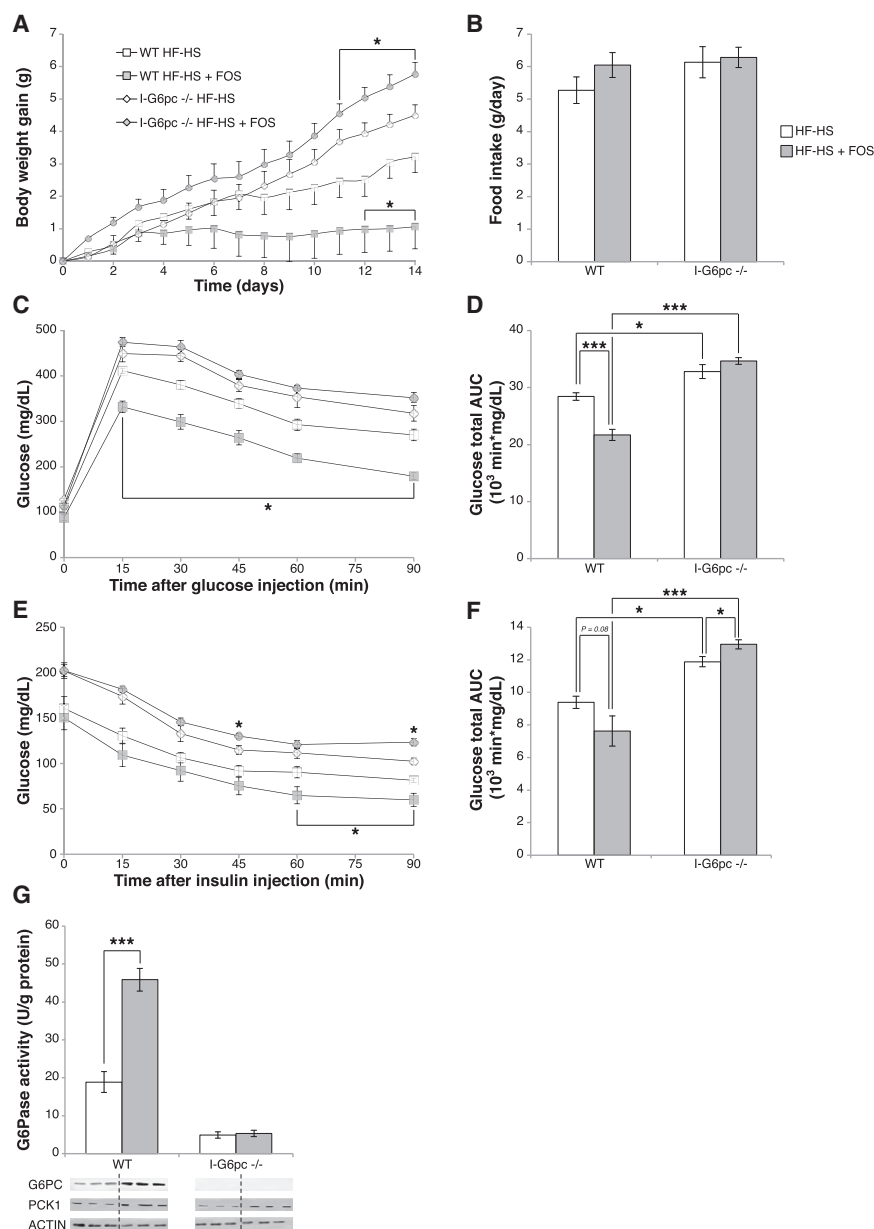
**Figure 6. Effect of FOS Enrichment on Body Weight and Glucose Homeostasis in WT and I-G6pc−/− Mice Fed a HF-HS Diet**

(A) Evolution of body weight gain in mice fed high-fat/high-sucrose (HF-HS) or FOS-supplemented (HF-HS + FOS) diet.

(B) Mean food intake over 2 weeks.

(C–F) Glucose (C) and insulin (E) tolerance tests were performed 16 and 18 days after switching to indicated diets, respectively. Total glucose areas under the curve (AUC) (D and F) were calculated.

(G) Effect of FOS enrichment on intestinal G6Pase activity in wild-type and I-G6pc−/− mice fed a high-fat/high-sucrose diet. Immunoblotting was performed to confirm the deletion.

*$p < 0.05$ (when not indicated versus HF-HS); ***$p < 0.001$, two-way ANOVA followed by Bonferroni's post hoc test. Data are mean ± SEM of n = 5 to 6 mice per group. WT, wild-type mice. See also Figure S5.

via an increase in cAMP and not via FFAR2 (Figures 3A–3C). An FFAR2-independent butyrate-initiated intracellular increase of cAMP has been described earlier in enterocytes and shown to be driven by the increase in ATP that accompanies utilization of butyrate as a key energy substrate (Wang et al., 2012). In contrast, we show that propionate acts as an agonist of FFAR3 in the periportal afferent neural system to induce IGN via a gut-brain neural circuit. The brain targets of the portal propionate signal include the DVC, which receive inputs from the ventral vagus nerve, and the C1 segment of the spinal cord and the PBN, which transmit inputs from the dorsal sympathetic ganglions and the spinal pathway. Such a double neural transmission has been observed for portal signals initiated by protein-digests via the μ-opioid receptors (Duraffourd et al., 2012). Thus, our data highlight the key role of the spinal pathway in nutrient signaling to the brain in addition to the vagal pathway, which is often considered as preponderant (Mithieux, 2013).

Beneficial effects of dietary fiber and SCFAs have been described in several studies, all showing resistance to diet-induced obesity and increased energy expenditure (Cani et al., 2007; Gao et al., 2009; Lin et al., 2012; Neyrinck et al., 2012). Propionate has long been described as a hepatic gluconeogenic substrate (Anderson and Bridges, 1984). However, here we show that propionate is converted into glucose by IGN (i.e., in the intestine before it reaches the liver). This promotes metabolic benefits in energy homeostasis, illustrated here through decreased adiposity and body weight despite comparable food intake, and better glucose control, including a decrease
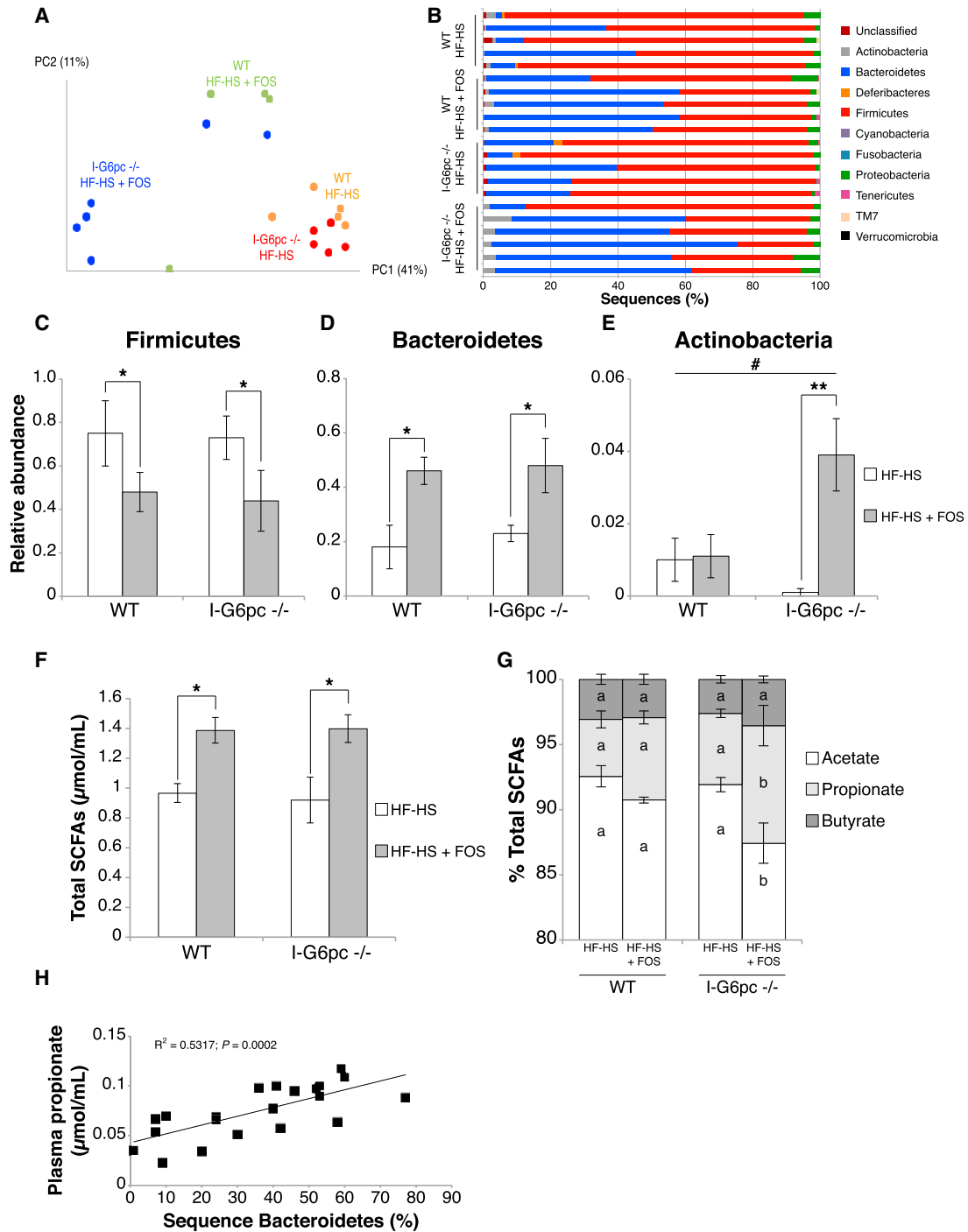
that SCFAs produced from microbial fermentation of polysaccharides improve various features of energy metabolism both in insulin-sensitive and insensitive states through stimulation of IGN. A major finding is that propionate can directly initiate a gut-brain neural circuit that has beneficial effects on host physiology.

SCFAs have been described as key signaling molecules, with activation of both FFAR2 and FFAR3 (preferentially activated by propionate) leading to modulation of host adiposity (Samuel et al., 2008) or GLP-1 secretion (Tolhurst et al., 2012). Here, we show that propionate and butyrate activate IGN genes using different and complementary processes. Our data suggest that butyrate directly activates IGN gene expression in enterocytes

**Figure 7. Effect of FOS-Enrichment on Colonic Microbiota Composition and Portal SCFAs in WT and I-G6pc−/− Mice Fed a HF-HS Diet**
(A) Principal coordinates analysis (PCoA) plot of unweighted UniFrac distances. Each dot represents a colonic community. The percentage of variation explained by each principal coordinate is shown in parentheses.
(B) Abundance plot of the most important phyla in each mouse.
(C–E) Relative abundance of phyla in the colonic microbiota.
(F and G). Total SCFA content in portal blood of mice fed regular high-fat/high-sucrose (HF-HS) or FOS-supplemented (HF-HS + FOS) diet (F) and SCFA proportions (G) in the portal blood of aforementioned mice.
(H) Bacteroidetes abundance positively correlates with the plasma propionate measured in the portal blood circulation.
*p < 0.05; **p < 0.01; # indicates statistical significance in the interaction between diet and mouse genotype; values with different letters differ significantly, two-way ANOVA followed by Bonferroni's post hoc test. Data are mean ± SEM of n = 5 to 6 mice per group. WT: Wild-type mice. See also Figure S6.

of hepatic glucose production, as described earlier (Mithieux et al., 2005, Troy et al., 2008). We directly confirmed the role of IGN in promoting the metabolic benefits of propionate by using I-G6pc−/− mice (i.e., mice that cannot convert propionate into glucose in the intestine), and show that metabolism is even slightly impaired by FOS feeding in these mice. We also show that FOS addition to a HF-HS diet increases the proportion of propionate in the total SCFA content in the portal blood of I-G6pc−/− mice. We thus propose that increased conversion of propionate into glucose by the liver contributes to the worsening of glucose tolerance in I-G6pc−/− mice.

Dietary fibers have been linked to marked alterations in the gut microbiota composition (Neyrinck et al., 2012). In addition, recent studies have shown a strong interaction between gut microbiota and host metabolism (El Aidy et al., 2013a, 2013b), including modulation of intestinal G6pc expression (Larsson et al., 2012, data available at http://microbiota.wall.gu.se). Here we show that the abundance of the two major phyla in the colonic microbiota is dramatically altered by FOS supplementation, regardless of the genetic background. FOS feeding increases the abundance of Bacteroidetes while decreasing the abundance of Firmicutes. Interestingly, the elevated levels of Bacteroidetes observed after FOS feeding strongly correlate with the increased levels of propionate in the plasma, confirming previous observations (Bindels et al., 2012). Although comparable changes in microbiota composition have been previously associated with beneficial effects for the host (Bindels et al., 2012; Roberfroid et al., 2010; Schwiertz et al., 2010; Turnbaugh et al., 2006), our data show that these changes are not sufficient to induce improvements in glucose and energy homeostasis in the absence of IGN. We also show that FOS feeding strongly increases the abundance of Actinobacteria, but only in I-G6pc−/− mice in which the beneficial effects of SCFAs or FOS are not observed. To date, we have no explanation for the link between FOS feeding and Actinobacteria levels, but as this association was not observed in WT mice, it is unlikely to have a role in the benefits linked to FOS feeding.

In conclusion, we report a mechanism linking microbial degradation of dietary fiber into SCFAs and host nutrient sensing through induction of IGN. We show that IGN has a causal role in the metabolic benefits that have long been ascribed to fiber-enriched diets. This reveals a key mechanistic rationale by which SCFAs, and especially propionate, may positively influence host metabolism. Since both the beneficial effects of dietary fiber on glucose control (Mendeloff, 1977; Ray et al., 1983; Robertson et al., 2003, 2005) and IGN (Battezzati et al., 2004; Hayes et al., 2011; Mithieux, 2012) are known to be present in humans, these findings may open novel perspectives in the treatment as well as prevention of metabolic diseases.

## EXPERIMENTAL PROCEDURES

### Animals

Adult male Sprague-Dawley rats (Charles River), aged 6 to 8 weeks and weighing 275–300 g at the time of their arrival, were housed in a climate-controlled room (22 ± 2°C) subjected to a 12 hr light/dark cycle (7:00 AM–7:00 PM), with free access to water and food. Mice were housed under similar conditions. I-G6pc−/− mice were generated as described previously (Penhoat et al., 2011), and experiments were performed 5 weeks after gene deletion.

Sodium propionate, sodium butyrate (Sigma) or FOS (Orafti P95, kindly donated by Beneo) was incorporated into the diet at 5% wt/wt (SCFAs) or 10% wt/wt (FOS). Standard diet was SAFE A04 (Augis, France) and HF-HS diet was prepared at Unité de Préparation des Aliments Expérimentaux (INRA Jouy-en-Josas, France; see also Table S1). Prior to diet change, animals were fed standard diet and groups were designed to match food intake and body weight.

### Glucose and Insulin Tolerance Tests

After 10 to 14 days of special or standard diet, animals were fasted for 16 (GTT) or 6 hr (ITT) and then received an injection of glucose (1 g/kg b.w., i.p.) or insulin (0.5 U/kg b.w., Insulatard, Novo Nordisk). Blood glucose was monitored for 90 min using a glucometer (Accu-Check, Roche) on samples collected from the tip of the tail vein. Insulin was quantified using an ELISA kit (Mercodia).

### Tissue Sampling

Rats were fasted for 6 hr and were then euthanized by pentobarbital injection (100 mg/kg b.w., i.p.). The intestine and liver were sampled as described previously (Mithieux et al., 2004a). G6Pase activity was assayed under maximal velocity conditions. Western blot was performed using antibodies described in Table S2, using β-actin as a housekeeping gene. All procedures were described in detail previously (Mithieux et al., 2004a; Rajas et al., 1999).

### Surgical Procedures

Rats were anesthetized with 2% isoflurane. Portal catheter implantation was performed as described earlier (Duraffourd et al., 2012). For portal denervation, a gauze compress moistened with either a capsaicin (10 mg/ml in saline, DMSO and Tween at a ratio of 8:1:1) or a vehicle solution was applied around the portal vein for denervation. Sodium propionate and β-hydroxybutyrate (Sigma) were dissolved in saline and perfused at a rate of 2.5 μmol/min for 6 hr in fasted rats. Rats were allowed to recover for 1 week, with free access to food and water. A marbocyl/ketofen solution was injected each day to prevent coagulation, infection, and pain.

### Determination of Intestinal Glucose Fluxes

After a 6 hr fast, rats were anesthetized with 2% isoflurane and fitted with polyethylene catheters inserted into the right jugular vein for [3-³H] glucose (Perkin-Elmer) infusion and the left carotid artery for blood sampling. For propionate incorporation studies, rats were fasted for 24 hr to enhance IGN (Mithieux et al., 2004b) and fitted with catheters as described above. [1-¹⁴C] Propionic acid sodium salt (Hartmann Analytic) was infused for 90 min. Sampling and calculations are described in detail by Croset et al. (2001).

### Immunofluorescence

Immunofluorescence was performed as described by Duraffourd et al. (2012), with prior incubation of slides in citrate buffer at 95°C for 40 min for antigen retrieval.

See also Table S1.

### c-Fos Labeling

Brain sampling, labeling, and counting are described in detail by Duraffourd et al. (2012).

### Sample Collection for Microbial and SCFA Analysis

Mice were fasted for 6 hr and euthanized by cervical dislocation. Blood samples were collected from the portal vein and via intracardiac puncture. The intestine (including the colon) and liver were sampled and immediately put in liquid nitrogen. For plasma analysis, blood samples were centrifuged and plasma collected and stored at −80°C before the assay.

### SCFA Assay

SCFAs were measured in 50 μl of plasma samples after acidification and extraction into diethyl ether by gas chromatograph coupled with mass spectrometer detector (7890A and 5975C, Agilent Technologies). A mix of 1 M [1-¹³C] acetate, 0.2 M [6-²H] propionate, and 0.2 M [4-¹³C] butyrate was added as internal standard. Prior to injection, the samples were derivatized with N-tert-butyldimethylsilyl-N-methyltrifluoroacetamide (MTBSTFA; Sigma) at

room temperature. Quantitation of the measured metabolites was completed in selected ion monitoring acquisition mode by comparison to labeled internal standards. The *m/z* ratios of monitored ions were as follows: 117 (acetic acid), 131 (propionic acid), 145 (butyric acid), 121 ([1-$^{13}$C]-acetate), 136 ([6-$^{2}$H] propionate), and 149 ([4-$^{13}$C] butyrate).

### Genomic DNA Purification, 16S rRNA Gene Amplification, and Sequence Analyses

After isolation of genomic DNA from colon segments (repeated bead-beating method, Salonen et al., 2010), the V1-V2 region of bacterial 16S rRNA gene was amplified using the 27F and 338R primers fused with 454 Titanium sequencing adapters. Three independent 25 μl PCR reactions were performed for each sample using 1.5 U of FastStart Taq DNA Polymerase (Roche) and PCR was performed at conditions: one cycle of 3 min at 95°C, 25 cycles: 20 s at 95°C, 30 s at 52°C, and 60 s at 72°C, and 10 min at 72°C. The resulting product was checked for size and purity on 0.8% Agarose-GelRed gel, further purified (NucleoSpin 740609, Macherey-Nagel, Germany), and quantified with the Quant-iT PicoGreen dsDNA kit (Invitrogen, Carlsbad, CA). All samples were pooled in equal amounts (20 ng/μl) and purified again with magnetic beads (AMPure XP, Beckman, Danvers, MA) to remove short amplification products. The purified pooled products were sequenced (Roche 454 GS-FLX system, Titanium chemistry, by GATC, Konstanz, Germany). 454 reads were denoised using the denoiser_preprocess.py and denoiser.py, tools available in QIIME and sequences were further analyzed as described in detail by Larsson et al. (2012). We retained 111,693 sequences for 21 mouse colon samples with an average of 5,320 sequences per sample (2,892 to 8,810 sequences). One of the colonic samples from a WT mouse on FOS diet contained a very low number of sequences (1,982 before denoising and 930 after); this sample was not included in the β-diversity analysis, but was included in all other analyses.

### Cell Culture

Caco-2 cells were purchased from ECACC and cultured as suggested by the supplier. The cells were seeded into 6-well plates at 10$^6$ cells/well and cultured at confluence at 37°C for 3 weeks. After that time, the culture medium was changed to Krebs-Ringer buffer with 1 mM sodium propionate, 1 mM tiglic acid, 1 mM 1-methylcyclopropanecarboxylic acid, or 1 mM sodium butyrate (Sigma) alone or in conjunction with 0.2 μg/ml pertussis toxin or 10 μM U73122 (Tocris). 24 hr later, cells were lysed for molecular analysis.

### cAMP Assay

cAMP in the lysates was quantified by a direct cAMP enzyme immunoassay kit according to the manufacturer's instructions (ENZO Life Sciences ADI-900-163). Protein concentrations of the lysates were determined using traditional Bradford assay. The concentration of cAMP was normalized to that of protein in the same lysates. A medium containing 10 μM forskolin was used as a positive control.

### Quantitative RT-PCR

Total RNA was extracted from frozen tissues and cells using Trizol reagent (Invitrogen), according to the manufacturer's instructions. Fast-Start SYBR Green PCR reagents (Roche) were used to determine mRNA levels. Ribosomal protein L19 (*RPL19*) was used as a housekeeping gene. Calculations were made based on the comparative cycle threshold method ($2^{-\Delta\Delta Ct}$). Primer sequences are given in Table S3.

### Statistical Analyzes

All data are presented as mean ± SEM. Two-group comparisons were analyzed using paired or unpaired t test. Groups were compared using one-way ANOVA followed by Tukey's (against all groups) and Dunnett's post hoc tests (against a control group). Two-way ANOVA followed by Bonferroni's post hoc test was used in experiments using I-G6pc−/− mice. The nonparametric Kruskal-Wallis test followed by Dunn's post hoc test was used for c-Fos neuron counting. $p < 0.05$ was considered as statistically significant.

## REFERENCES

Anderson, J.W., and Bridges, S.R. (1984). Short-chain fatty acid fermentation products of plant fiber affect glucose metabolism of isolated rat hepatocytes. Proc. Soc. Exp. Biol. Med. *177*, 372–376.

Battezzati, A., Caumo, A., Martino, F., Sereni, L.P., Coppa, J., Romito, R., Ammatuna, M., Regalia, E., Matthews, D.E., Mazzaferro, V., and Luzi, L. (2004). Nonhepatic glucose production in humans. Am. J. Physiol. Endocrinol. Metab. *286*, E129–E135.

Berthoud, H.-R. (2004). Anatomy and function of sensory hepatic nerves. Anat. Rec. A Discov. Mol. Cell. Evol. Biol. *280*, 827–835.

Bindels, L.B., Porporato, P., Dewulf, E.M., Verrax, J., Neyrinck, A.M., Martin, J.C., Scott, K.P., Buc Calderon, P., Feron, O., Muccioli, G.G., et al. (2012). Gut microbiota-derived propionate reduces cancer cell proliferation in the liver. Br. J. Cancer *107*, 1337–1344.

Brown, A.J., Goldsworthy, S.M., Barnes, A.A., Eilert, M.M., Tcheang, L., Daniels, D., Muir, A.I., Wigglesworth, M.J., Kinghorn, I., Fraser, N.J., et al. (2003). The Orphan G protein-coupled receptors GPR41 and GPR43 are activated by propionate and other short chain carboxylic acids. J. Biol. Chem. *278*, 11312–11319.

Cani, P.D., Neyrinck, A.M., Fava, F., Knauf, C., Burcelin, R.G., Tuohy, K.M., Gibson, G.R., and Delzenne, N.M. (2007). Selective increases of bifidobacteria in gut microflora improve high-fat-diet-induced diabetes in mice through a mechanism associated with endotoxaemia. Diabetologia *50*, 2374–2383.

Clore, J.N., Stillman, J., and Sugerman, H. (2000). Glucose-6-phosphatase flux in vitro is increased in type 2 diabetes. Diabetes *49*, 969–974.

Croset, M., Rajas, F., Zitoun, C., Hurot, J.M., Montano, S., and Mithieux, G. (2001). Rat small intestine is an insulin-sensitive gluconeogenic organ. Diabetes *50*, 740–746.

Cummings, J.H., Pomare, E.W., Branch, W.J., Naylor, C.P., and Macfarlane, G.T. (1987). Short chain fatty acids in human large intestine, portal, hepatic and venous blood. Gut *28*, 1221–1227.

Delaere, F., Duchampt, A., Mounien, L., Seyer, P., Duraffourd, C., Zitoun, C., Thorens, B., and Mithieux, G. (2012). The role of sodium-coupled glucose co-transporter 3 in the satiety effect of portal glucose sensing. Mol Metab *2*, 47–53.

Donohoe, D.R., Garge, N., Zhang, X., Sun, W., O'Connell, T.M., Bunger, M.K., and Bultman, S.J. (2011). The microbiome and butyrate regulate energy metabolism and autophagy in the mammalian colon. Cell Metab. *13*, 517–526.

Duraffourd, C., De Vadder, F., Goncalves, D., Delaere, F., Penhoat, A., Brusset, B., Rajas, F., Chassard, D., Duchampt, A., Stefanutti, A., et al. (2012). Mu-opioid receptors and dietary protein stimulate a gut-brain neural circuitry limiting food intake. Cell 150, 377–388.

El Aidy, S., Derrien, M., Merrifield, C.A., Levenez, F., Doré, J., Boekschoten, M.V., Dekker, J., Holmes, E., Zoetendal, E.G., van Baarlen, P., et al. (2013a). Gut bacteria-host metabolic interplay during conventionalisation of the mouse germfree colon. ISME J. 7, 743–755.

El Aidy, S., Merrifield, C.A., Derrien, M., van Baarlen, P., Hooiveld, G., Levenez, F., Doré, J., Dekker, J., Holmes, E., Claus, S.P., et al. (2013b). The gut microbiota elicits a profound metabolic reorientation in the mouse jejunal mucosa during conventionalisation. Gut 62, 1306–1314.

Flint, H.J., Scott, K.P., Louis, P., and Duncan, S.H. (2012). The role of the gut microbiota in nutrition and health. Nat Rev Gastroenterol Hepatol 9, 577–589.

Gao, Z., Yin, J., Zhang, J., Ward, R.E., Martin, R.J., Lefevre, M., Cefalu, W.T., and Ye, J. (2009). Butyrate improves insulin sensitivity and increases energy expenditure in mice. Diabetes 58, 1509–1517.

Gautier-Stein, A., Zitoun, C., Lalli, E., Mithieux, G., and Rajas, F. (2006). Transcriptional regulation of the glucose-6-phosphatase gene by cAMP/vasoactive intestinal peptide in the intestine. Role of HNF4alpha, CREM, HNF1alpha, and C/EBPalpha. J. Biol. Chem. 281, 31268–31278.

Hayes, M.T., Foo, J., Besic, V., Tychinskaya, Y., and Stubbs, R.S. (2011). Is intestinal gluconeogenesis a key factor in the early changes in glucose homeostasis following gastric bypass? Obes. Surg. 21, 759–762.

Hidalgo, I.J., Raub, T.J., and Borchardt, R.T. (1989). Characterization of the human colon carcinoma cell line (Caco-2) as a model system for intestinal epithelial permeability. Gastroenterology 96, 736–749.

Hildebrandt, M.A., Hoffmann, C., Sherrill-Mix, S.A., Keilbaugh, S.A., Hamady, M., Chen, Y.-Y., Knight, R., Ahima, R.S., Bushman, F., and Wu, G.D. (2009). High-fat diet determines the composition of the murine gut microbiome independently of obesity. Gastroenterology 137, 1716–1724, e1–e2.

Karlsson, F.H., Tremaroli, V., Nookaew, I., Bergström, G., Behre, C.J., Fagerberg, B., Nielsen, J., and Bäckhed, F. (2013). Gut metagenome in European women with normal, impaired and diabetic glucose control. Nature 498, 99–103.

Kimura, I., Inoue, D., Maeda, T., Hara, T., Ichimura, A., Miyauchi, S., Kobayashi, M., Hirasawa, A., and Tsujimoto, G. (2011). Short-chain fatty acids and ketones directly regulate sympathetic nervous system via G protein-coupled receptor 41 (GPR41). Proc. Natl. Acad. Sci. USA 108, 8030–8035.

Larsson, E., Tremaroli, V., Lee, Y.S., Koren, O., Nookaew, I., Fricker, A., Nielsen, J., Ley, R.E., and Bäckhed, F. (2012). Analysis of gut microbial regulation of host gene expression along the length of the gut and regulation of gut microbial ecology through MyD88. Gut 61, 1124–1131.

Layden, B.T., Angueira, A.R., Brodsky, M., Durai, V., and Lowe, W.L., Jr. (2013). Short chain fatty acids and their receptors: new metabolic targets. Transl. Res. 161, 131–140.

Lin, H.V., Frassetto, A., Kowalik, E.J., Jr., Nawrocki, A.R., Lu, M.M., Kosinski, J.R., Hubert, J.A., Szeto, D., Yao, X., Forrest, G., and Marsh, D.J. (2012). Butyrate and propionate protect against diet-induced obesity and regulate gut hormones via free fatty acid receptor 3-independent mechanisms. PLoS ONE 7, e35240.

Lozupone, C., and Knight, R. (2005). UniFrac: a new phylogenetic method for comparing microbial communities. Appl. Environ. Microbiol. 71, 8228–8235.

Magnusson, I., Rothman, D.L., Katz, L.D., Shulman, R.G., and Shulman, G.I. (1992). Increased rate of gluconeogenesis in type II diabetes mellitus. A 13C nuclear magnetic resonance study. J. Clin. Invest. 90, 1323–1327.

Mendeloff, A.I. (1977). Dietary fiber and human health. N. Engl. J. Med. 297, 811–814.

Mithieux, G. (2012). Comment about intestinal gluconeogenesis after gastric bypass in human in relation with the paper by Hayes et al., Obes. Surg. 2011. Obes. Surg. 22, 1920–1922, author reply 1923–1924.

Mithieux, G. (2013). Nutrient control of hunger by extrinsic gastrointestinal neurons. Trends Endocrinol. Metab. 24, 378–384.

Mithieux, G., Bady, I., Gautier, A., Croset, M., Rajas, F., and Zitoun, C. (2004a). Induction of control genes in intestinal gluconeogenesis is sequential during fasting and maximal in diabetes. Am. J. Physiol. Endocrinol. Metab. 286, E370–E375.

Mithieux, G., Rajas, F., and Gautier-Stein, A. (2004b). A novel role for glucose 6-phosphatase in the small intestine in the control of glucose homeostasis. J. Biol. Chem. 279, 44231–44234.

Mithieux, G., Misery, P., Magnan, C., Pillot, B., Gautier-Stein, A., Bernard, C., Rajas, F., and Zitoun, C. (2005). Portal sensing of intestinal gluconeogenesis is a mechanistic link in the diminution of food intake induced by diet protein. Cell Metab. 2, 321–329.

Mutel, E., Gautier-Stein, A., Abdul-Wahed, A., Amigó-Correig, M., Zitoun, C., Stefanutti, A., Houberdon, I., Tourette, J.-A., Mithieux, G., and Rajas, F. (2011). Control of blood glucose in the absence of hepatic glucose production during prolonged fasting in mice: induction of renal and intestinal gluconeogenesis by glucagon. Diabetes 60, 3121–3131.

Neyrinck, A.M., Possemiers, S., Verstraete, W., De Backer, F., Cani, P.D., and Delzenne, N.M. (2012). Dietary modulation of clostridial cluster XIVa gut bacteria (Roseburia spp.) by chitin-glucan fiber improves host metabolic alterations induced by high-fat diet in mice. J. Nutr. Biochem. 23, 51–59.

Nøhr, M.K., Pedersen, M.H., Gille, A., Egerod, K.L., Engelstoft, M.S., Husted, A.S., Sichlau, R.M., Grunddal, K.V., Poulsen, S.S., Han, S., et al. (2013). GPR41/FFAR3 and GPR43/FFAR2 as cosensors for short-chain fatty acids in enteroendocrine cells vs FFAR3 in enteric neurons and FFAR2 in enteric leukocytes. Endocrinology 154, 3552–3564.

Parks, B.W., Nam, E., Org, E., Kostem, E., Norheim, F., Hui, S.T., Pan, C., Civelek, M., Rau, C.D., Bennett, B.J., et al. (2013). Genetic control of obesity and gut microbiota composition in response to high-fat, high-sucrose diet in mice. Cell Metab. 17, 141–152.

Penhoat, A., Mutel, E., Amigo-Correig, M., Pillot, B., Stefanutti, A., Rajas, F., and Mithieux, G. (2011). Protein-induced satiety is abolished in the absence of intestinal gluconeogenesis. Physiol. Behav. 105, 89–93.

Pillot, B., Soty, M., Gautier-Stein, A., Zitoun, C., and Mithieux, G. (2009). Protein feeding promotes redistribution of endogenous glucose production to the kidney and potentiates its suppression by insulin. Endocrinology 150, 616–624.

Rajas, F., Bruni, N., Montano, S., Zitoun, C., and Mithieux, G. (1999). The glucose-6 phosphatase gene is expressed in human and rat small intestine: regulation of expression in fasted and diabetic rats. Gastroenterology 117, 132–139.

Ray, T.K., Mansell, K.M., Knight, L.C., Malmud, L.S., Owen, O.E., and Boden, G. (1983). Long-term effects of dietary fiber on glucose tolerance and gastric emptying in noninsulin-dependent diabetic patients. Am. J. Clin. Nutr. 37, 376–381.

Roberfroid, M., Gibson, G.R., Hoyles, L., McCartney, A.L., Rastall, R., Rowland, I., Wolvers, D., Watzl, B., Szajewska, H., Stahl, B., et al. (2010). Prebiotic effects: metabolic and health benefits. Br. J. Nutr. 104 (Suppl 2), S1–S63.

Robertson, M.D., Currie, J.M., Morgan, L.M., Jewell, D.P., and Frayn, K.N. (2003). Prior short-term consumption of resistant starch enhances postprandial insulin sensitivity in healthy subjects. Diabetologia 46, 659–665.

Robertson, M.D., Bickerton, A.S., Dennis, A.L., Vidal, H., and Frayn, K.N. (2005). Insulin-sensitizing effects of dietary resistant starch and effects on skeletal muscle and adipose tissue metabolism. Am. J. Clin. Nutr. 82, 559–567.

Sagar, S.M., Sharp, F.R., and Curran, T. (1988). Expression of c-fos protein in brain: metabolic mapping at the cellular level. Science 240, 1328–1331.

Salonen, A., Nikkilä, J., Jalanka-Tuovinen, J., Immonen, O., Rajilić-Stojanović, M., Kekkonen, R.A., Palva, A., and de Vos, W.M. (2010). Comparative analysis of fecal DNA extraction methods with phylogenetic microarray: effective recovery of bacterial and archaeal DNA using mechanical cell lysis. J. Microbiol. Methods 81, 127–134.

Samuel, B.S., Shaito, A., Motoike, T., Rey, F.E., Bäckhed, F., Manchester, J.K., Hammer, R.E., Williams, S.C., Crowley, J., Yanagisawa, M., and Gordon, J.I. (2008). Effects of the gut microbiota on host adiposity are modulated by the